COMBUSTION CHARACTERISTICS AND MIGRATION BEHAVIOR OF NUCLIDES DURING INCINERATION OF LOW-LEVEL RADIOACTIVE WASTE

by

Renhui RUAN[a], Guan WANG[a], Wenjing MA[a], Jianyu LI[b], Ao ZHOU[a], Jie LU[b], Minghui YANG[b], Yi CHEN[b], Houzhang TAN[a], and Xuebin WANG[a*]

[a]MOE Key Laboratory of Thermo-Fluid Science and Engineering, School of Energy and Power Engineering, Xi'an Jiaotong university, Xi'an, Shaanxi, China
[b]China Nuclear Power Technology Research Institute Co., Ltd, Shen Zhen, Guangdong, China

Original scientific paper
https://doi.org/10.2298/TSCI230212162R

Incineration is a main method of disposal low-level radioactive waste (LLRW). However, the combustion characteristics and migration of nuclides during incineration is still unclear. This study first investigated the effect of package mass, feeding time interval, air distribution, and water vapor supply on the combustion characteristics of LLRW and NO_x emission. Optimal parameters were obtained based on combustion efficiency and NO_x concentration. Then, the migration of nuclides was studied in conditions with the optimal parameters. The results showed that the combustion efficiency and NO_x concentration were affected by furnace temperature, redox atmosphere and their distribution inside the furnace. Package mass, feeding time interval, and air distribution were optimized to balance the thermal decomposition rate of the waste and the oxidation rate of the combustible gas generated from thermal decomposition of the waste. Water vapor supply can decrease the furnace temperature and the thermal decomposition rate of the waste. The optimal parameters of package mass, feeding time interval, air distribution, and the feeding rate of water vapor is 100 g/bag, 40 seconds, 0.5/0.23/0.23/0.23 (excess air coefficient) for the first layer to fourth layer of air inlet, and 25 kg per hours, respectively. During incineration, more than 99% nuclides were fixed in bottom ash. The order of the ratio of nuclides in flue gas, fly ash, and bottom ash is bottom ash > flue gas > fly ash. Based on the ratio of nuclides in fly ash and flue gas, the order of volatility of nuclides during incineration is Cr > C s> Mn > Co > Nb > Zr.

Key words: *LLRW, incineration, nuclides, burnout rate, NO_x*

Introduction

The GHG from the utilization of fossil fuel will cause global warming. To realize carbon neutrality, it is necessary to increase the proportion of renewable and sustainable energy [1]. Because solar and wind energy are intermittent and large-scale energy storage is not ready by now, we still need to rely on thermal power plants with high flexibility or nuclear energy

*Corresponding author, e-mail: wxb005@mail.xjtu.edu.cn

[2]. However, increasing amount of radioactive wastes are produced from nuclear energy. Among them, the amount of LLRW are the largest [3, 4]. Improper disposal of LLRW will release radionuclides into the environment, threatening human health and damaging the environment [5].

Incineration is a mainstream technology to deal with high proportion of rubber and plastic solid waste, especially for LLRW [6, 7]. Since the 1960's, incineration technology with excess air was first developed. This resulted in a low combustion efficiency and high pollutant emission. To solve these problems, CILVA in Belgium, Los Alamos in USA, and Envikraft proposed air-staged combustion for LLRW [8]. The waste was first combusted in a primary combustion chamber (PCC) closed to the theoretical excess air coefficient, and then the residual air was supplied into the secondary combustion chamber (SCC) to complete the combustion. In this way, flue gas has a more residence time in high temperature zone, which can increase high burnout rate. Besides, air-staged combustion can reduce NO_x emission [9]. Based on that, the China Institute for Radiation Protection (CIRP) developed a pyrolytic-incineration technology in the 1990's [10]. In conventional combustion, the pyrolysis process overlaps with the combustion process. In pyrolysis-incineration technology, fuel first undergoes thermal decomposition and partly combustion under fuel-rich atmosphere with a high temperature. Char and combustible gas are produced. Later, residual air is suppled to complete combustion. These combustion technologies are similar to preheating combustion or air-staged combustion of pulverized coal. The basic idea is to control the combustion intensity and increase the residence time of flue gas in reductive atmosphere [11-13].

During the incineration of LLRW, part of the radioactive nuclides can vaporize at high temperature. Rest of the radioactive nuclides will transfer into bottom ash. When flue gas cools down, part of the gaseous radioactive nuclides will condense on the surface of fly ash or the surface of heat exchanger. Generally, the incinerator is equipped with air pollution control device to remove nuclides from flue gas. The migrations of radioactive nuclides during incineration of LLRW have been investigated. The CIRP [14] found that when treated by hot plasma between 1100 °C and 1400 °C, temperature has no significant effect on the capture of radioactive nuclides. A higher content of Cl will decrease the capture of Co and Cs, while has no effect on the capture of Sr. Wang *et al*. [15] used thermal equilibrium method to investigate the migration of nuclides during thermal decomposition of LLRW. It was found that Co and Sr did not vaporize during pyrolysis of LLRW. When the gasification temperature is below 1200 ºC, the vaporization of Co and Sr can be prevented. Yang and Kim [16] dispose LLRW in a plasma arc melting furnace and studied the vaporization of Co and Cs. A significant vaporization of Cs was observed. The distribution of nuclides in flue gas and vitreous slag is affected by the composition of solid waste and the initial nuclides concentrations. Dmitriev *et al*. [17] used plasma gasification and melting technology to dispose radioactive waste. The concentration of ^{137}Cs, ^{60}Co, and U in flue gas can be reduced by optimization of the furnace. Nakashima *et al*. [18] found that with an increase of the alkalinity of the melting ash, the proportion of ^{137}Cs in molten ash decreased while the solidification of ^{60}Co by molten ash was not affected. Oshita *et al*. [19] studied the migration of Cs during incineration of model waste. It was found that with an increase of temperature and excess air coefficient, the proportion of Cs in ash increased and Cs mainly existed as chlorides. Jiao *et al*. [20] studied the vaporization of water-soluble Cs during heat treatment of Cs-containing ash. Addition of $CaCl_2$ and $MgCl_2$ can increase the vaporization of Cs by formation of Cs chloride. Fujiwara *et al*. [21] studied the migration of Cs during the incineration of solid waste produced in the decontamination process of Fukushima nuclear accident. Different from published research, the content of Cs in bottom ash and fly ash is close

to each other. Therefore, the migration of radioactive nuclides during incineration of LLRW is complicated and needs further investigation.

This work studied the combustion characteristics and migration of nuclides in a self-designed incinerator. The effect of package mass, feeding time interval, air distribution, and water vapor supply on the combustion characteristics of model waste and NO_x emission were investigated. The migration of nuclides was also studied under the optimal conditions.

Experimental section

Properties of samples

According to the compositions of LLRW from a nuclear power plant in China, a model waste was prepared by mixing polyethylene (PE) and cotton cloth (CC) with a mass ratio of 3:2. The ultimate and proximate analysis of PE and CC are shown in tab. 1. Figure 1 shows the real LLRW from a nuclear power plant and the model waste in experiment.

Table 1. Proximate and ultimate analysis of model waste

		PE	CC			PE	CC
Proximate analysis				Ultimate analysis			
M_{ar}	wt.%	0.15	1.28	C_d	wt.%	85.83	60.62
A_{ar}	wt.%	0.05	0.83	H_d	wt.%	13.77	5.05
V_{ar}	wt.%	99.80	95.40	O_d	wt.%	0.00	31.97
FC_{ar}	wt.%	0.00	0.83	N_d	wt.%	0.09	0.08
$Q_{net,ar}$	MJ/kg	43.2	19.9	S_d	wt.%	0.110	0.170

Note: ar – as received, d – dry basis, M – moisture, A – ash, V – volatile, FC – fixed carbon, Q_{net} – low heating value

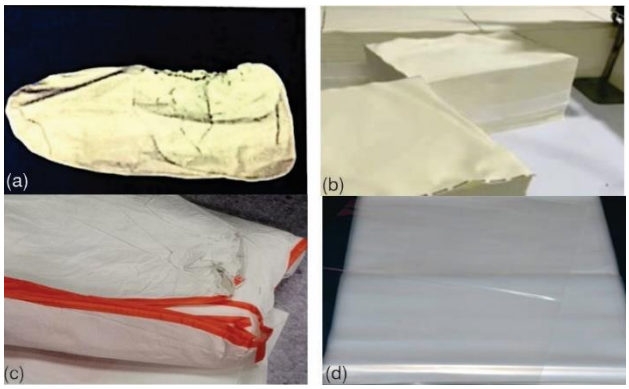

Figure 1. Real LLRW; (a) and (c) from a nuclear power plant and the model waste and (b) and (d) in experiment

The specific activity of nuclides in real LLRW from a nuclear power plant is shown in tab. 2. Nuclides including Co, Nb, Mn, Cr, Zr, and Cs were investigated in this study because they contribute more than 96% of the specific activity in the real LLRW. Nitrates of nuclides were dissolved in de-ionized water and then sprayed on the surface of the model waste. The mass content of each nuclide in the model waste is 0.16% in experiment.

Experimental system and sampling methods

The incineration system includes an incinerator, a water vapor generator, and air pollution control devices. The sampling system include gas analyzer and fly ash sampling device.

Incinerator

The incinerator consists of a PCC, a SCC, and a grate as shown in figs. 2 and 3. The PCC contains four layers of air inlet, with one layer below the grate and three layers above the grate, tab. 3. Water vapor can be supplied from the air inlet below the grate. As shown in fig.

3, the temperature of PCC and SCC is measured by a thermocouple, fly ash and flue gas were sampled at the outlet of PCC.

Table 2. Specific activity of nuclides in LLRW

Nuclides	Activity contribution [%]	Specific activity [Bqkg^{-1}]	Nuclides	Activity contribution [%]	Specific activity [Bqkg^{-1}]
^{58}Co	48.47	1.94×10^{6}	^{14}C	0.09	3.87×10^{3}
^{60}Co	9.67	3.87×10^{5}	^{63}Ni	2.90	1.16×10^{5}
^{95}Nb	14.51	5.81×10^{5}	^{90}Sr	0.12	4.65×10^{3}
^{54}Mn	9.67	3.87×10^{5}	^{94}Nb	2.89×10^{-5}	1.16×10^{2}
^{51}Cr	4.84	1.94×10^{5}	^{99}Tc	1.45×10^{-5}	5.81×10^{1}
^{95}Zr	4.84	1.94×10^{5}	^{129}I	7.27×10^{-6}	2.91×10^{1}
^{137}Cs	4.84	1.94×10^{5}			

Generator of water vapor

The generator of water vapor consists of a water vapor heater and an air heater. De-ionized water was used to generate water vapor.

Fly ash sampling and flue gas analyzing

As shown in fig. 2, fly ash was sampled at the inlet of SCC and collected by quartz filter (MK 360, Munktell, Sweden). The concentration of O_2, CO, and NO_x in flue gas was analyzed by a gas analyzer (Testo 350) at the inlet of SCC.

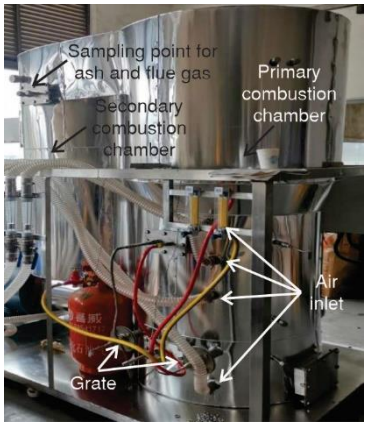

Figure 2. Incinerator of model LLRW

Sampling of nuclides

Nuclides were sampled at the inlet of SCC. The sampling system is shown in fig. 4 according to US EPA Method 29 [22]. Fly ash in the flue gas was filter by quartz membrane. Then, gaseous nuclides were absorbed by absorption liquid in impinger with ice bath. The first impinger was left empty for condensation of flue gas. The second and third impinger contain 200 ml absorption liquid (5%V/V HNO_3 and 10%V/V H_2O_2). The last impinger contains silica gel to dry the flue gas. Bottom ash was also sampled to analyze the concentration of nuclides.

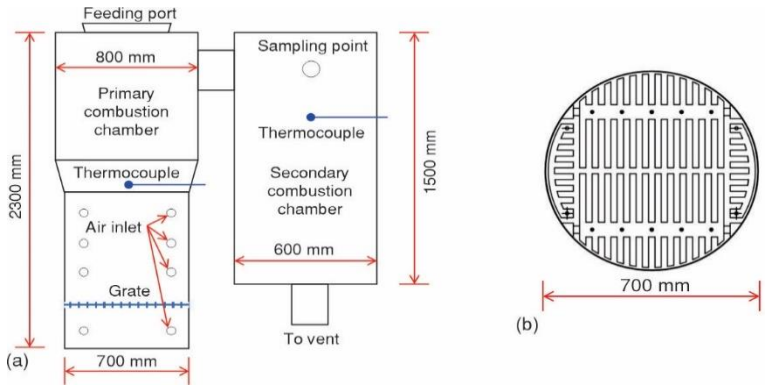

Figure 3. Schematic of the incinerator and the grate; (a) schematic of the incinerator and (b) schematic of the grate

Table 3. Air distribution for each layer of air inlet

Layer of air inlet	Case					
	#1	#2	#3	#4	#5	#6
First layer	0.3	0.4	0.5	0.6	0.7	1.2
Second layer	0.3	0.26	0.23	0.2	0.16	0
Third layer	0.3	0.26	0.23	0.2	0.16	0
Fourth layer	0.3	0.26	0.23	0.2	0.16	0

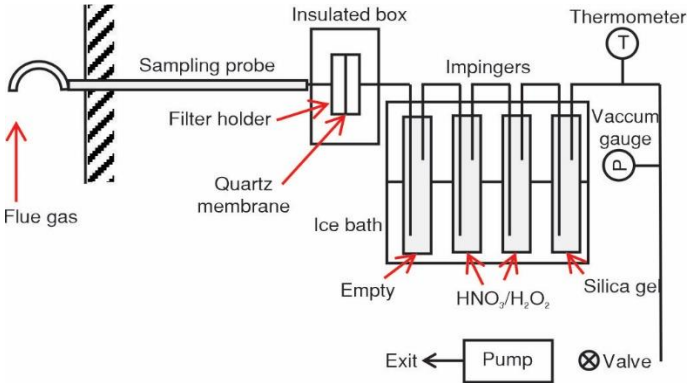

Figure 4. Sampling system of radioactive nuclides according to US EPA Method 29 [22]

Characterization method

Concentration of fly ash

The quartz membrane was dry at 105 ℃ and then weighted before and after sampling to obtain the mass of fly ash. The concentration of fly ash was obtained by dividing the mass of fly ash by the cumulative volume of flue gas passing through the quartz membrane.

Mass loss rate of fly ash

Fly ash on quartz membrane was calcined at 500 ℃ till a constant weight in muffle furnace to get the mass loss rate of fly ash.

Concentration of nuclides

The concentrations of nuclides in fly ash, absorption liquid, and bottom ash were analyzed by an Inductively Coupled Plasma-Mass Spectrometer (ICP-MS, NexION 350D, PerkinElmer), according to China Standard HJ 766–2015.

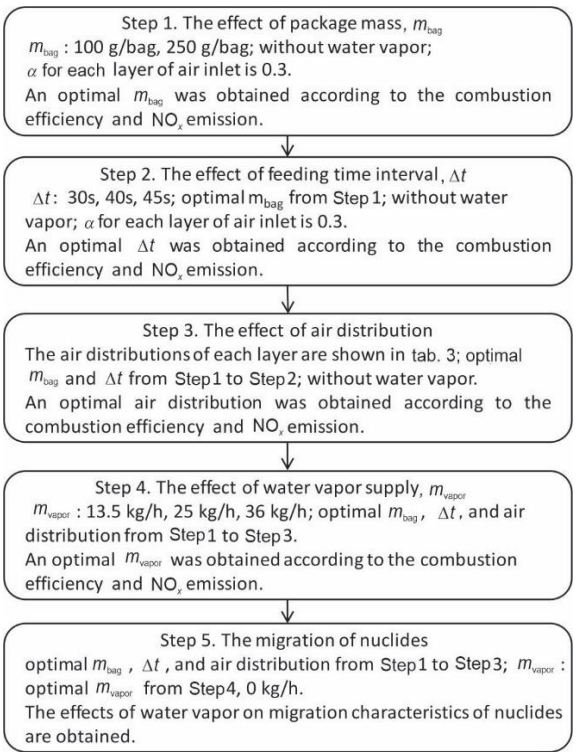

Figure 5. Experimental conditions.

Experiment conditions

The furnace was heated up by natural gas and then the model waste was fed from top of PCC with a constant time interval. The temperature of PCC, SCC, and the grate were recorded. The total excess air coefficient, α, is 1.2. The effects of package mass, m_{bag}, feeding time interval, Δt, air distribution, and water vapor supply, m_{vapor}, on the combustion characteristics and NO_x emission were studied. Optimal parameters were obtained based on the experiment result. Then, the migration of nuclides was conducted in condition with the optimal parameters. The experiment conditions are shown in fig. 5.

Results and discussion

The effect of package mass, m_{bag}

Figure 6 shows the temperature range of the PCC, SCC, and grate with different m_{bag}. When m_{bag} is 100 g/bag, the temperature of PCC is lower, and the fluctuation of temperature is smaller than 250 g/bag. After the package is fed from top of the PCC, it undergoes thermal decomposition and partly combustion. The combustion of the combustible gas occurs when it is gradually mixed with the residual air from the second layer to fourth layer of air inlet. When m_{bag} is 250 g/bag, the concentration of combustible gas inside PCC is higher than that of 100 g/bag. More heat will be released from oxidation of the combustible gas inside PCC. Therefore ,the temperature inside PCC is higher and the fluctuation of temperature is larger. However, higher temperature will accelerate the corrosion of metal parts of inside the furnace [23]. Therefore, the optimal m_{bag} is 100 g/bag.

The effect of feeding time interval, Δt

Figure 7 shows the temperature range of PCC, SCC, and grate with different Δt. After the package is fed into PCC, the temperature of PCC first increases and then decreases. With an increase of Δt, PCC has more time to cool down. Therefore, increasing Δt will decrease the temperature of PCC and increase the temperature fluctuation. Besides, the combustion rate in PCC is slower with a longer Δt, and the flame inside PCC will moves towards a higher position. This will increase the temperature of SCC. Therefore, increasing Δt will increase the temperature of SCC. However, Δt has no obvious effect on the grate temperature.

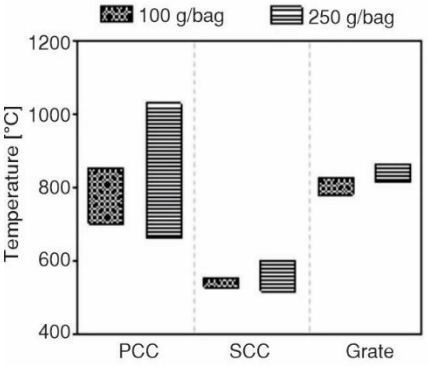

Figure 6. Temperature of PCC, SCC, and grate with different m_{bag}

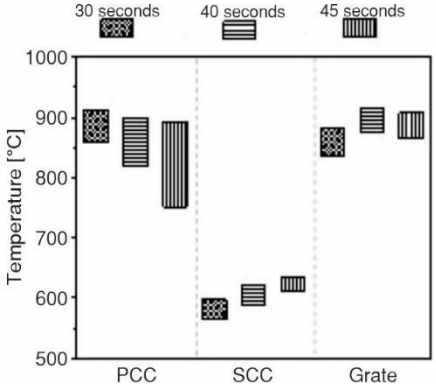

Figure 7. Temperature of PCC, SCC, and grate with different Δt

Figure 8 shows the CO concentration at the inlet of SCC with different Δt. With an increase of Δt, CO concentration decreases first and then increases. The CO concentration is

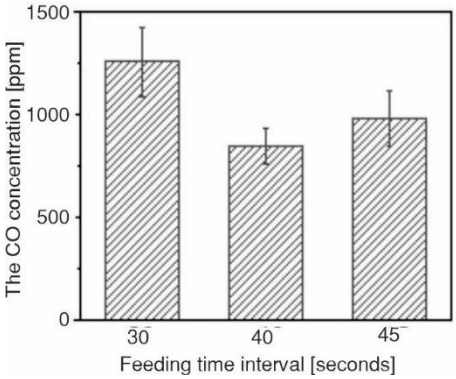

Figure 8. The CO concentration at inlet of SCC with different Δ*t*

determined by the oxidation of the combustible gas from decomposition of the package. A higher furnace temperature results in a higher decomposition rate of the package, a higher oxidation rate of the combustible gas and a shorter residence time in furnace. A higher decomposition rate of package and a shorter residence time will increase CO concentration while a higher oxidation rate of the combustible gas will decrease CO concentration. As shown in fig. 7, when Δ*t* increases from 30 seconds to 45 seconds, temperature of PCC increases. It indicates that the relationship between temperature of PCC and CO concentration is non-monotonical. The highest burnout rate can be achieved when Δ*t* is 40 seconds for this incinerator.

The effect of air distribution

Figure 9 shows the temperature range of the PCC, SCC, and grate with different air distribution. For different cases, the temperature range of PCC is similar. For SCC, with an increase of α below the grate, SCC temperature first increases and then decreases. Air distribution has no obvious effect on the grate temperature.

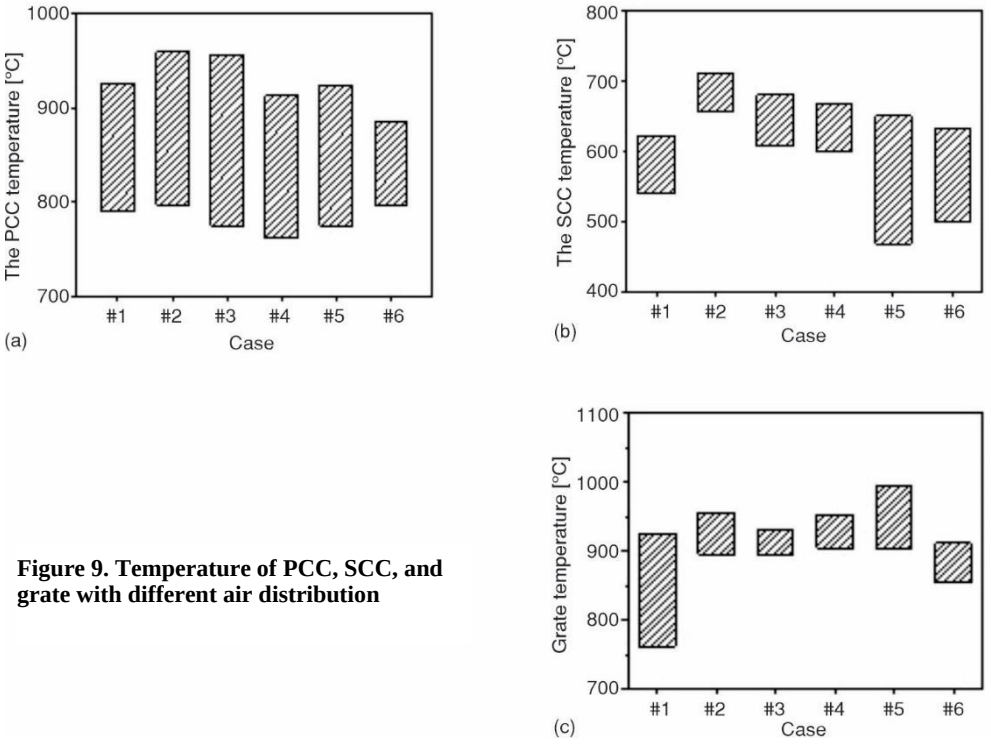

Figure 9. Temperature of PCC, SCC, and grate with different air distribution

Figure 10 shows the concentration of CO and NO_x with different air distribution. The concentration of CO and NO_x is lowest in Case #3. The redox atmosphere and the distribution

of furnace temperature can be tuned by changing air supply. This is similar to the adjustment of secondary air and over-fire air in coal-fired power plant [24, 25]. According to Zeldovich model, eqs. (1)-(4), [26], the formation of thermal NO_x is strongly positively correlated with O_2 concentration and temperature. Because the temperature of PCC is lower than 1000 ℃, there would be no thermal NO_x. If all of the fuel-N is converted to NO_x, the theoretical NO_x concentration would be 245 mg/Nm^3. However, NO_x concentrations with different air distributions are all lower than 245 mg/Nm^3, confirming that NO_x mainly comes from the fuel-N. Conditions with a high temperature and efficient oxygen will increase NO_x concentration, while conditions with a low temperature and insufficient oxygen will decrease the burnout rate. Reasonable control of temperature and oxygen concentration is important to achieve a high burnout rate and low NO_x emission. According to the concentration of CO and NO_x, the optimal air distribution is Case #3:

$$O_2 \rightleftarrows O+O \tag{1}$$

$$N_2+O \rightleftarrows NO+N \tag{2}$$

$$N+OH \rightleftarrows NO+H \tag{3}$$

$$R_{NO} = 3\times10^{14} C_{N_2} C_{O_2}^{1/2} \exp\left(-542000/RT\right) \tag{4}$$

where R_{NO} is the formation rate of NO_x, C_{N2} and C_{O2} are concentration of N_2 and O_2, and T is the temperature.

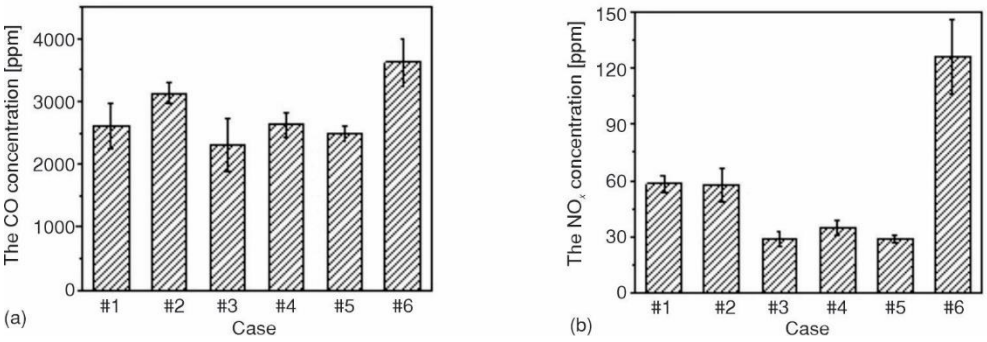

Figure 10. The CO (a) and NOx (b) concentration at inlet of SCC with different air distribution

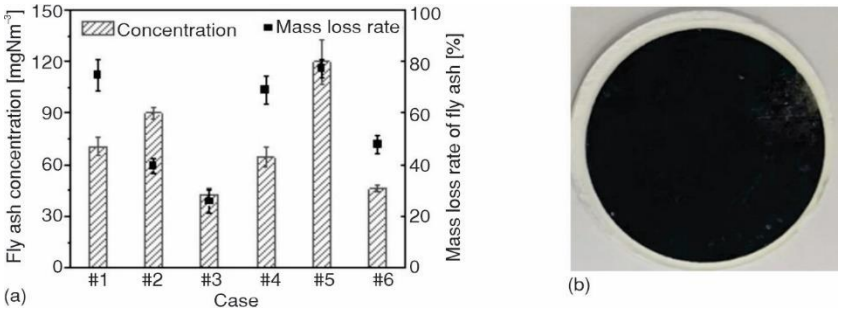

Figure 11. Concentration, mass loss rate, and morphology of fly ash with different air distribution; (a) concentration and mass loss rate of the fly ash and (b) morphology of fly ash

Figure 11 shows the concentration, mass loss rate, and morphology of fly ash. The fly ash is black, indicating that it contains a lot of unburned matter. The unburned matter could be soot from aromatization of thermal decomposition products of fuel at high temperature. The concentration and mass loss rate of fly ash is lowest in Case #3. Therefore, the optimal air distribution is Case #3.

The effect of water vapor supply

Figure 12 shows the temperature of PCC, SCC, and grate with different water vapor supply, m_{vapor}. Water vapor can absorb heat inside PCC and decrease PCC temperature. With an increase of m_{vapor}, PCC temperature decreases. Water vapor can also effectively decrease grate temperature, which can protect grate from serious corrosion. However, water vapor has no obvious effect on SCC temperature.

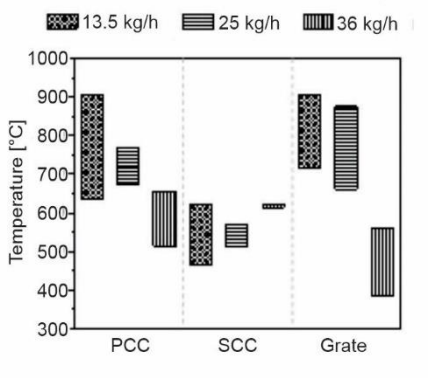

Figure 12. Temperature of PCC, SCC, and grate with different m_{vapor}

Figure 13 shows the concentration of CO and NO_x at inlet of SCC with different m_{vapor}. Combustion efficiency is affected by the rate of formation and oxidation of the combustible gas generated from decomposition of the waste. Supply of water vapor can decrease PCC temperature, which will decrease the decomposition rate of the waste and the oxidation rate of combustible gas. A high or low m_{vapor} will decrease the combustion efficiency. Therefore, CO centration is lowest when m_{vapor} is 25 kg/h. Results in fig. 13 show that NO_x concentration is lowest when m_{vapor} is 25 kg/h.

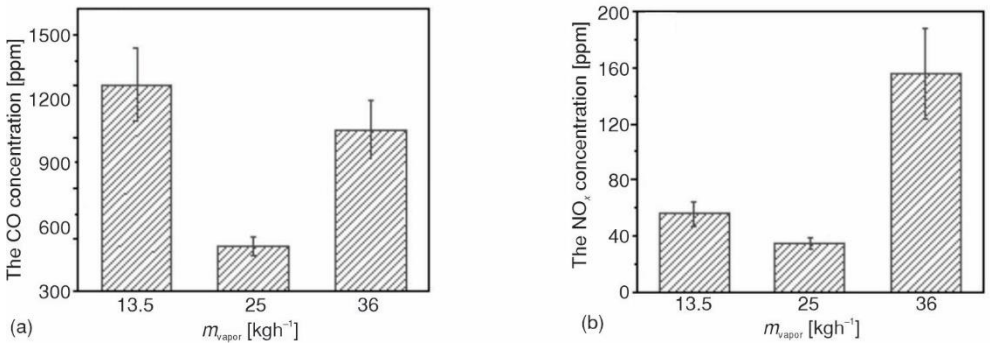

Figure 13. The CO (a) and NO_x (b) concentration at inlet of SCC with different m_{vapor}

Figure 14 shows the concentration and mass loss rate of the fly ash with different m_{vapor}. Water vapor can decrease the concentration of fly ash while has no obvious effect on the mass loss rate of the fly ash. According to the furnace temperature, concentration of CO and NO_x, and the concentration of fly ash, the optimal m_{vapor} is 25 kg/h.

The migration of nuclides

Tables 4 and 5 shows the distribution of nuclides in flue gas, fly ash, and bottom ash with and without water vapor supply. The order of the distribution ratio of nuclides is bottom

ash > flue gas > fly ash. More than 99% of the nuclides are distributed in bottom ash. A water vapor supply of 25 kg/h can increase the ratio of nuclides in fly ash while has no obvious effect on the ratio of nuclides in flue gas. A higher ratio of nuclides in fly ash and flue gas indicates a higher volatility. The order of the volatility of nuclides is Cr > Cs > Mn > Co > Nb ≈ Zr. Nuclides are transformed to fly ash by vaporization and subsequently condensation, which is similar to the gas-to-particle transformation of inorganic elements during coal combustion [27]. Water vapor supply will decrease the furnace temperature and enhance the reductive atmosphere by gasification of water vapor and the waste. A higher temperature or a stronger reductive atmosphere can increase the vaporization of nuclides [27]. The experiment results show that temperature rather than reductive atmosphere dominates the vaporization of nuclides during incineration.

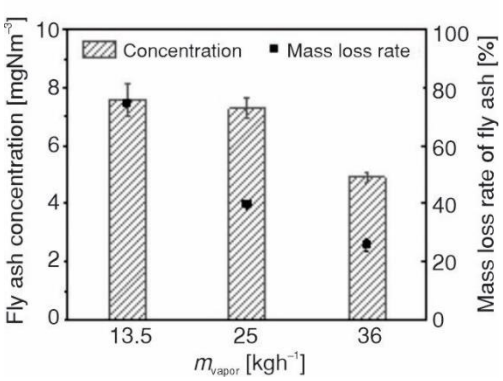

Figure 14. Concentration and mass loss rate of the fly ash with different m_{vapor}

Table 4. Distribution of nuclides in flue gas, fly ash, and bottom ash when m_{vapor} is 25 kg/h

	Cr	Mn	Co	Zr	Nb	Cs
Flue gas	0.4356	0.1064	0.0819	0.0167	0.0390	0.3766
Fly ash	0.2420	0.0815	0.0513	0.0817	0.0491	0.1174
Bottom ash	99.3225	99.8122	99.8668	99.9016	99.9119	99.5060

Table 5. Distribution of nuclides in flue gas, fly ash, and bottom ash when m_{vapor} is 0 kg/h

	Cr	Mn	Co	Zr	Nb	Cs
Flue gas	0.4571	0.1146	0.0837	0.0190	0.0382	0.3464
Fly ash	0.1071	0.0050	0.0016	0.0064	0.0015	0.1155
Bottom ash	99.4358	99.8804	99.9147	99.9746	99.9603	99.5381

Conclusions

This study focused on the combustion characteristics and migration of nuclides during incineration of LLRW. The effect of package mass, feeding time interval, air distribution, and water vapor supply on the combustion characteristics of LLRW and NO_x emission were investigated. The migration of nuclides was also studied. The results can help understand the combustion process and pollutants migration during incineration of LLRW. Besides, it is useful to the design and operation of incinerator of LLRW. The main conclusions are as follows.

- To increase the combustion efficiency and decrease NO_x concentration, the distribution of temperature and redox atmosphere need to be tuned to balance the thermal decomposition rate of the waste and the oxidation rate of the combustible gas. The optimal package mass and feeding time interval is 100 g/bag and 40 seconds, respectively. The optimal excess air coefficient for the first layer to the fourth layer of air inlet is 0.5, 0.23, 0.23, and 0.23, respectively.
- Water vapor supply can decrease the furnace temperature and the decomposition rate of the waste. Combustion efficiency is affected by the formation rate of combustible gas generated

from decomposition of the waste and the oxidation rate of the combustible gas. The optimal water vapor supply is 25 kg/h.

- The order of the ratio of nuclides in flue gas, fly ash, and bottom ash is bottom ash > flue gas > fly ash. More than 99% of nuclides is fixed in bottom ash. Water vapor supply can increase the ratio of nuclides in fly ash while has no obvious effect on the ratio of nuclides in flue gas. The order of volatility of nuclides is Cr > Cs > Mn > Co > Nb ≈ Zr. Temperature rather than reductive atmosphere dominates the vaporization of nuclides during incineration of LLRW.

Acknowledgment

This research was supported by the National Natural Science Foundation of China (No. 52206170), Innovative Scientific Program of CNNC, the Postdoctoral Research Foundation of China (No. 2021M702570) and the National Key R&D Program of China (No. 2018YFB1900203).

References

[1] Pleßmann, G., *et al*., Global Energy Storage Demand for a 100% Renewable Electricity Supply. *Energy Procedia*, *46* (2014), Dec., pp. 22-31
[2] Gonzalez-Salazar, M. A., *et al*., Review of the Operational Flexibility and Emissions of Gas- and Coal-Fired Power Plants in a Future with Growing Renewables, *Renewable and Sustainable Energy Reviews*, *82* (2018), Part 1, pp. 1497-1513
[3] Kim, M., *et al*., Leaching Behaviors and Mechanisms of Vitrified Forms for the Low-Level Radioactive Solid Wastes, *Journal of Hazardous Materials*, *384* (2020), 121296
[4] Afgan, N., Sustainable Nuclear Energy Dilemma, *Thermal Science*, *17* (2013), 2, pp. 305-321
[5] Adeola A., *et al*., Advances in the Management of Radioactive Wastes and Radionuclide Contamination in Environmental Compartments: A Review, *Env. Geo. and Health, 45* (2022), Sept., pp. 2663-2689
[6] Brems, A., *et al*., Recycling and Recovery of Post-Consumer Plastic Solid Waste in a European Context, *Thermal Science, 16* (2012), 3, pp. 669-685
[7] Tochaikul, G., *et al*., Radioactive Waste Treatment Technology: A Review, *Kerntechnik, 87* (2022), 2, pp. 208-225
[8] Hultgren A., Reprocessing of Spent Nuclear Fuels. Status and Trends (in Sweden), Report No. STUDSVIK-NS-93-5, Nykoping, Sweden, 1993
[9] Houshfar, E., *et al*., Effect of Excess Air Ratio and Temperature on NO_x Emission from Grate Combustion of Biomass in the Staged Air Combustion Scenario, *Energy & Fuels*, *25* (2011), 10, pp. 4643-4654
[10] Xu, W., *et al*., Application and Improvement of Low & Medium-Level Radioactive Waste Pyrolysis Incineration Technology in China, *Radiation Protection, 40* (2020), 5, pp. 387-393
[11] Ouyang, Z., *et al*., Experimental Study on Combustion, Flame and NO_x Emission of Pulverized Coal Preheated by a Preheating Burner, *Fuel Processing Technology*, *179* (2018), Oct., pp. 197-202
[12] Wang, M., *et al*., Numerical Simulation on the Emission of NO_x from the Combustion of Natural Gas in the Sidewall Burner, *Thermal Science, 26* (2022), 1A, pp. 247-258
[13] Zhu, S., *et al*., Pilot-Scale Study on NO Emissions from Coarse Coal Combustion Preheated by Circulating Fluidized Bed, *Fuel*, *280* (2020), 118563
[14] Jiang, Y., *et al*., Experimental Analysis on Solidification of Simulated Organic Low-Level Radioactive Waste by Thermal Plasma, *High Voltage Engineering*, *39* (2013), 7, pp. 1750-1756
[15] Wang, H. W., *et al*., Evaluation on Migration and Transformation of Trace Nuclides in Thermal Degradation for Low-Level Radioactive Waste, *Journal of Analytical and Applied Pyrolysis*, *161* (2022), 105420
[16] Yang, H. C., Kim, J. H., Characteristics of Dioxins and Metals Emission from Radwaste Plasma Arc Melter System, *Chemosphere*, *57* (2004), 5, pp. 421-428
[17] Dmitriev SA., *et al*., Plasma Plant for Radioactive Waste Treatment, *Proceedings*, WM'01 Conference, Tucson, Ariz., USA, 2001, pp. 1-10
[18] Nakashima, M., *et al*., Characterization of Solidified Products Yielded by Plasma Melting Treatment of Simulated Non-Metallic Radioactive Wastes, *Journal of Nuclear Science and Technology*, *39* (2002), 6, pp. 687-694

[19] Oshita K., *et al*., Behavior of Cesium in Municipal Solid Waste Incineration, *Journal of Environmental Radioactivity, 143* (2015), May, pp. 1-6
[20] Jiao, F., *et al*., Role of $CaCl_2$ and $MgCl_2$ Addition in the Vaporization of Water-Insoluble Cesium from Incineration Ash During Thermal Treatment, *Chemical Engineering Journal, 323* (2017), Sept., pp. 114-123
[21] Fujiwara H., *et al*., Behavior of Radioactive Cesium During Incineration of Radioactively Contaminated Wastes from Decontamination Activities in Fukushima, *Journal of Environmental Radioactivity*, *178-179* (2019), Nov., pp. 290-296
[22] Zhao, S., *et al*., Migration and Emission Characteristics of Trace Elements in a 660 MW Coal-Fired Power Plant of China, *Energy & Fuels*, *30* (2016), 7, pp. 5937-5944
[23] Xiong, X., *et al*., Investigation on High Temperature Corrosion of Water-Cooled Wall Tubes at a 300 MW Boiler, *Journal of the Energy Institute*, *93* (2020), 1, pp. 377-386
[24] Wang, Q., *et al*., Effects of Secondary Air Distribution in Primary Combustion Zone on Combustion and NO Emissions of a Large-Scale Down-Fired Boiler with Air Staging, *Energy*, *165* (2018), Part B, pp. 399-410
[25] Hodzic, N., *et al*., Influence of Over Fire Air System on NO_x Emissions: An Experimental Case Study, *Thermal Science, 23* (2019), 3B, pp. 2037-2045
[26] Hill, S. C., Smoot, L. D., Modeling of Nitrogen Oxides Formation and Destruction in Combustion Systems, *Progress in Energy and Combustion Science, 26* (2000), 4-6, pp. 417-458
[27] Quann, R. J., Sarofim, A. F., Vaporization of Refractory Oxides During Pulverized Coal Combustion. *Symposium (International) on Combustion*, *19* (1982), 1, pp. 1429-1440

Paper submitted: February 12, 2023
Paper revised: June 20, 2023
Paper accepted: June 21, 2023